PERIODICA POLYTECHNICA SER. CIV. ENG. VOL. 49, NO. 1, PP. 27–46 (2005)

CONDITION MONITORING OF A LIGHTLY REINFORCED CONCRETE BEAM BY DYNAMIC MEASUREMENTS

Tamás KOVÁCS and György FARKAS

Department of Structural Engineering
Budapest University of Technology and Economics
H–1521 Budapest, Hungary
e-mails: kovacst@vbt.bme.hu, farkas@vbt.bme.hu

Received: April 7, 2005

Abstract

The paper deals with the assessment of damage in a lightly reinforced concrete beam using the measured values of the first natural frequency. The aim of the presented laboratory experiment was the experimental investigation of the relationship between the degree of cracking and the first natural frequency under defined deterioration conditions. As a result of the test, a definite relationship between the investigated parameters could be demonstrated.

Keywords: vibration, natural frequency, excitation, amplitude-spectrum, bending stiffness.

1. Introduction

1.1. Background

During the design life of the existing concrete (mainly bridge-) structures unfavourable serviceability conditions occur due to various corrosive effects and actions coming from extreme traffic loads, what may lead to insufficient load bearing capacity. Early detection of these deterioration processes is the most important task of the maintenance. One of the possible ways to do this is the regular observation of the change in the dynamic characteristics. If the mass, the geometric dimensions and the bearing conditions are constant in the course of time, change in the bending stiffness or in the normal (prestressing) force induces a change in the dynamic characteristics. Discontinuities in the material due to cracks cause change in the degree of the 'internal friction', what leads to a change in the damping characteristics.

Most of the existing concrete bridges are subjected to bending or to the combination of compression and bending. The reasons of the degradation in the bending stiffness are the decreasing cross section of the reinforcement due to corrosion, the degradation in the structure of concrete due e.g. to freezing, the decreasing prestressing force due to the ruptures of tendons and the developing cracks.

1.2. The Aim of the Research Programme

Many research projects focus on the application of dynamic parameters to characterize the structural behaviour of concrete structures under different service conditions [1], [2]. In most of these cases the modal parameters such as the natural frequencies, the mode shapes of the vibration and possibly the damping ratio are measured by a non-destructive diagnostic technique in order to perform some kind of 'structural condition evaluation' [3], [4], [5]. The essence of these methods is to point out changes in these quantities and then to use them for accessing the degree of damage accumulated in the structure due to the above degradation processes, e.g. cracking, steel corrosion, prestressing tendon ruptures etc. [6]. For [3] and [4] an equivalent moment of inertia was calculated as a damage identification parameter that established a relation between the degree of the accumulated damage in the model beams caused by the artificially produced cracks and the measured natural frequencies.

In some cases, these methods cannot be effectively used, especially in cases when no relevant comparable result of the measured dynamic quantity is available from past investigations, and when the exact localization of the defect of the structure is expected.

As a possible answer to the first difficulty, our research programme aims to find numerical relationship between the easily measurable dynamic characteristics and the quantities characterizing the degree of deterioration of a structure as a whole by performing laboratory test series at the laboratory of the Budapest University of Technology, Department of Structural Engineering. As a preliminary work to this programme, in-situ dynamic measurements have been carried out on existing concrete bridges in order to check the previously measured values of the dynamic characteristics and to investigate the applicability of the normal road traffic as an excitation action during the dynamic measurements. The expected result of this research programme is the development of the conditions for the continuous monitoring of concrete bridges based on their dynamic characteristics in order to be able to follow the typical deterioration processes during the full design life of the structures.

This paper deals with a small part of this programme by presenting a laboratory experiment carried out on a lightly reinforced concrete beam. As a consequence, its results can be considered as a particular case from the point of view of the whole project.

1.3. Excitation Possibilities

In real situations, the first few natural frequencies are aimed to determine [2]. In laboratory conditions it is possible to apply harmonic excitation. In this case, continuously changing the excitation frequency, resonance effects appear in the vibration pattern (in the recorded deflection-time or acceleration-time function), which indicate the equality of the excitation and one of the natural frequencies. For

on site investigations, the frequency range of the excitation has to be wide enough to contain all the natural frequencies to be determined and secondly, the intensities of the amplitudes in the amplitude-frequency function of the excitation have to be sufficiently high at the frequencies close to the natural frequencies of the structure in order to produce a significant excitation effect in that frequency ranges.

For dynamic measurements carried out on existing reinforced concrete bridges, for practical reasons, the approximation of the so-called Dirac-δ effect (*Fig.1*) and that of a perfect impulse effect (*Fig. 2*) are mostly used as artificially produced excitations.

The subfigures in *Fig. 1* and *Fig. 2* show the theoretical amplitude-time ($A-t$) functions of the above two excitation effects. The excitation effect occurs at the moment of time when the amplitude of the excitation begins to change according to the subfigures and has an influence on the structure while this change takes place. Theoretically, the magnitude of the amplitude of the Dirac-δ impulse is infinite ($A = \infty$) and the lengths of the periods of these amplitude-changes according to the subfigures in *Fig. 1* and *Fig. 2* are zero ($\Delta t = 0$). However in real situations, these type of excitations cannot be carried out for practical reasons, i.e. this $A \neq \infty$ and $\mathrm{d}t \neq 0$ naturally. For in-situ measurements, the approximation of these excitations can be generated by impact effects (*Fig. 1*) and by applying objects falling on or off the examined structure (*Fig. 2*) respectively.

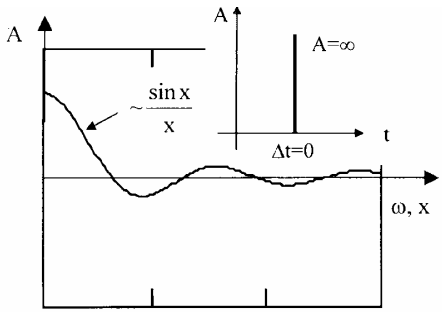

Fig. 1. Excitation function of Dirac-δ

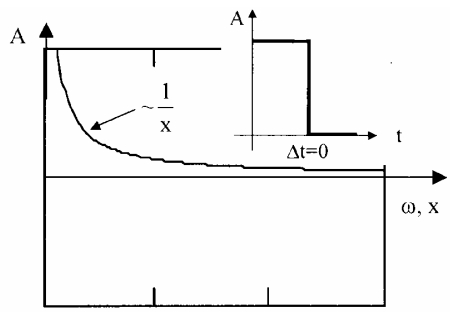

Fig. 2. Ideal (diminishing) impulse excitation

The main diagrams in *Fig. 1* and *Fig. 2* show the frequency ranges ($A-\omega$) of the above two types of excitation describing the functions between the intensity of the exciting effect (A) and the excited frequency (ω). This function can be approximated by a $\sin(x)/x$ function for the Dirac-δ effect (*Fig. 1*) and by a $1/x$ function for the impulse effects (*Fig. 2*), where x is an independent variable. It can be seen in *Fig. 1* and *Fig. 2* that for both cases, the intensity of the excitation is much higher in the lower frequency domains compared to that in the higher frequency domains. As a consequence of this, these excitations can be applied in the first place for determining the first few natural frequencies.

For highway bridges the road traffic is frequently used for excitation. The wide amplitude-spectrum of the exciting effect comes from the non-uniform running-

properties of different vehicles crossing the bridge. Because of the stochastic character of this excitation, it is necessary to evaluate the results in statistical way based on a sufficiently long time interval. Doing this, the excitation frequencies, which are not close enough to any of the natural frequencies, will occur in random manner and will be sifted out from the vibration pattern. Those, which are close to one of the natural frequencies, will amplify the weight of the free vibration in the vibration pattern.

1.4. Preliminary In-Situ Dynamic Measurements on Concrete Highway Bridges

Dynamic measurements have been carried out on existing reinforced concrete highway bridges in order to investigate the applicability of the normal road traffic as an excitation effect, to check the previously measured values of the natural frequencies and to gain experiences on the measurement possibilities of damping using the normal road traffic for excitation. The essence of this measuring and evaluating method was the assumption of a stochastic character for the exciting effect. The dynamic characteristics came out from statistical analysis, for which sufficient amount of measuring data were registered on site. The experiences got from this field can be summarized as follows:

- Using the normal road traffic for excitation and based on the on-site-recorded, sufficiently long acceleration-time functions, the average amplitude spectrums [7] can be produced in statistical way, which have significant peak-ordinates. Based on the resulting spectrums derived from combining these average amplitude spectrums, the first three natural frequencies and the belonging mode shapes could easily be determined [8].
- Determination of the logarithmic decrement of damping based on the excitation caused by the normal road traffic was performed by selecting parts from the on-site registered acceleration-time function of vibration, which represented a roughly free vibration. The logarithmic decrement of damping had been determined individually on these parts then the individual values (assumed as a representative sample) were analysed statistically. The statistical analysis resulted in high standard distribution values because of the difficulties of selecting periods from the registered acceleration-time function representing free vibration. After the statistical analysis of the mentioned representative samples containing sufficiently large number of data, the logarithmic decrement value could be given in an interval with a relative frequency of ~ 0.01 instead of a definite numerical value [9].

2. Laboratory Tests

In order to determine a relationship between the first natural frequency and the current states of deterioration under defined conditions, simply supported, reinforced

and prestressed concrete model beams have been investigated. All the model beams had the same concrete cross section (*Fig. 3*) whose nominal and real geometrical data can be seen in *Fig. 4*. The length of beams was 3.6 m for the R1, R2, P2, P2p marked specimens and 3.2 m for the P1 marked specimen. According to *Fig. 3*, the test specimens had different types of reinforcement and different steel ratios. The specimens marked with R1 and R2 contained reinforcing steel, the P1 and P2 marked specimens contained unstressed prestressing wires and the P2p marked specimens contained the same reinforcement as the P2 specimens but the wires in P2p specimen were pre-tensioned.

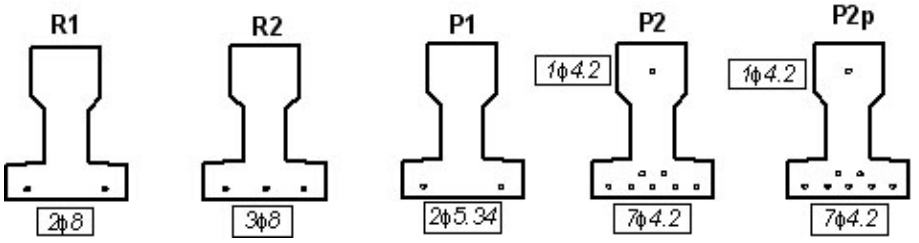

Fig. 3. Cross sections of the test specimens

Altogether three specimens have been investigated for each type with the exception of P1, in this case only one specimen has been analysed. Currently the evaluation of the experimental results is in progress.

In the following the investigation of the P1 marked specimen will be introduced [10], [11]. Because of the low reinforcement ratio (*Table 3*), the P1 marked specimen can be considered as a lightly reinforced concrete beam similar to many of the existing concrete bridges. For real reinforced concrete bridges, which have no prestressing, the design requirements concerning the deformation of the structure (e.g. deflection limits for beam girders) make necessary to provide sufficient (bending) stiffness and, as a consequence, larger geometric dimensions compared to load-bearing structures used for buildings, which results in relatively low reinforcement ratios. This fact significantly influences the behaviour of structures both for cracked stages under service conditions and for stages close to failure. Despite investigating only one P1 type specimen, which therefore can be considered as a preliminary test from the point of view of the whole research programme, this experimental programme regarding the number of the artificially produced cracked stages as well as the number of the dynamic measuring phases were chosen in such a way that it was possible to observe tendencies and to establish conclusions.

2.1. Geometrical and Material Properties

The tested specimen was originally a precast, prestressed concrete product with constant concrete section along the full length and with 7 prestressing wires in

the tension zone and with 1 wire in the compression zone (type P2p in *Fig. 3*). However, for this experimental purpose, it was manufactured only with 2, unstressed prestressing wires in the tension zone along the full length. The cross section and the side view of the specimen as well as their nominal and checked real geometric dimensions can be seen in *Fig. 4*, *Table 1* and *Fig. 5*.

Table 1. Geometric dimensions

Geometric dimensions of the P1 specimen [mm]				
	Real sizes			Nominal size
	One end	Other end	Mean value	
h	190.0	188.0	189.0	190
b_c	80.0	79.1	79.6	80
b_w	49.5	50.7	50.1	50
h_c	60.7	61.2	61.0	60
h_t	41.0	42.9	42.0	45
b_t	140.0	145.2	142.6	140
a	21.4	20.0	20.7	20
L			3190	3200
k			85	100

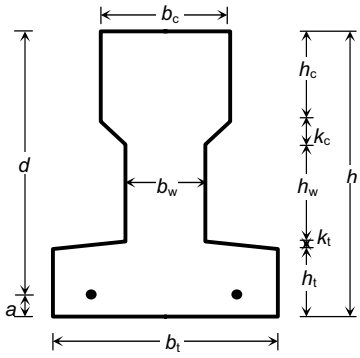

Fig. 4. Geometric dimensions (notations)

The applied mean values of the material properties are based on the EC-2 and can be found in *Table 2*. The design values of the strengths (f_{cd}, f_{pd}) including the partial safety of the resistance side according to the EC-2 was also determined and given in *Table 2*. In calculating the mean tensile strength of the prestressing steel, the coefficient of variation of strength was assumed as 10%, beside a normal probability distribution.

Table 2. Material properties

Concrete: C35/40 ($f_{ck} = 35$ N/mm^2)	Design value	Mean value
Compressive strength $f_{cd} = f_{ck}/1.5$; $f_{cm} = f_{ck} + 8$ [N/mm^2]	23.3 (f_{cd})	43
Mean value of the flexural tensile strength $f_{ctm.fl} = 2 \times 0.3\, f_{ck}^{2/3}$ [N/mm^2]		6.42
Short-term modulus of elasticity, $E_{cm} = 9500(\, f_{ck}$[N/mm^2] $+ 8)^{1/3}$ [N/mm^2]		33500
Prestressing steel: 1770-5.34 ST ($f_{pk} = 1770$ N/mm^2)		
Diameter, ϕ [mm]	5.34	
Tensile strength $f_{pd} = 0.9\, f_{pk}/1.15$, and $f_{pm} = f_{pk}(1 + 1.645 \times 0.1)$ [N/mm^2]	1385 (f_{pd})	2061
Modulus of elasticity, E_p [N/mm^2]	195000	

For calculating the bending capacity of the beam, a horizontal top branch was taken into account to the stress-strain curve of the prestressing steel, the shape of the stress-strain diagram of concrete was assumed to be rectangular with an ultimate compressive strain (ε_{cu}) of 0.35% according to the EC-2. Using the mean values of material properties given in *Table 2* and the geometric dimensions of the real cross section given in *Table 1* and *Fig. 4*, the mean value of the bending capacity (M_{Rm}) and the cracking moment (M_{cr}) as well as the reinforcement ratio (μ) based on the total concrete section (A_c) and on the width of the web (b_w) were calculated. The results can be found in *Table 3*, where d is the effective depth of the cross section. The design bending capacity based on the design strengths (f_{cd}, f_{pd}) given in *Table 2* and the nominal cross sectional dimensions given in *Table 1* and *Fig. 4* resulted in $M_{Rd} = 9.33$ kNm.

Table 3. Calculated properties of the cross section

	Based on the real cross section
Bending capacity, M_{Rm} [kNm]	14.08
Cracking moment, M_{cr} [kNm]	4.47
Reinforcement ratio [%]	
$\mu = A_s/A_c$	0.287
$\mu = A_s/(b_w d)$	0.531

2.2. Experimental Arrangement and Programme

For modelling a deterioration process, different cracking states were produced in 7 different loading steps by a four-point bending test (*Fig.5*, *Table 4*).

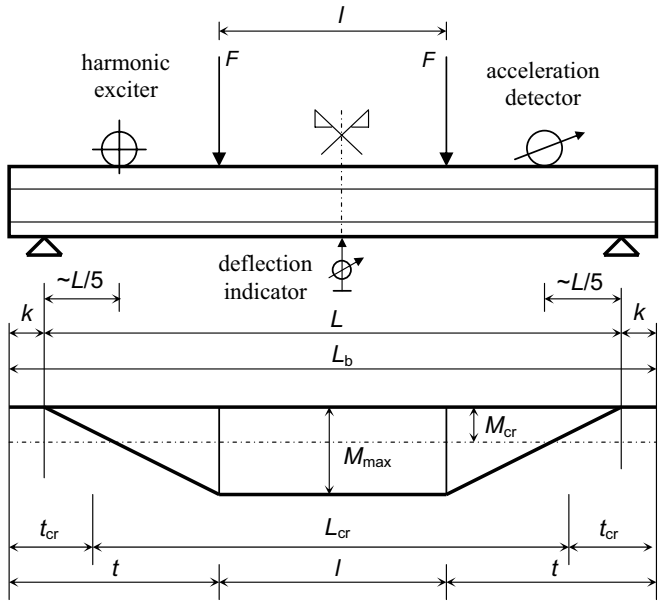

Fig. 5. Arrangement of the four-point bending test

The acting forces (F) were equal to each other and symmetric to the midspan in each load position.

Table 4. Loading properties of the deterioration states

Mark of the deterioration state	Load		Length of the cracked zone	Utilization for bending at the middle section	
	F [kN]	l [m]	L_{cr} [m]	$M_{\max}/M_{Rm}$	$M_{\max}/M_{Rd}$
0	0	–	0	0.035	0.054
1	5.13	0.5	1.59	0.52	0.80
2	6.63	1.0	1.94	0.55	0.84
31	8.13	1.5	2.16	0.52	0.79
32	11.13	1.5	2.42	0.71	1.07
4	9.63	1.0	2.42	0.78	1.19
5	11.13	0.5	2.42	1.10	1.66

In the loading steps number 1, 2 and 31 the length of the cracked zone (L_{cr}) had been gradually increased on approximately the same level of utilization for bending at the middle section then, beside constant length for the cracked zone, the utilization for bending was increased. Only the self weight (g_0=0.39 kN/m) loaded the specimen in the loading step number 0 while the maximum load was applied to the beam in the loading step number 5 getting the middle section close to failure. *Table 4* contains data related to the exact values and the positions of the acting forces as well as to the lengths of the cracked zone calculated on the basis of the cracking moment (M_{Rm}) given in *Table 3*. Values of utilization for bending at the middle section as a value of $M_{\max}/M_{Rm}$ are also added in this table. The $M_{\max}/M_{Rd}$ ratios give the values of utilization based on the design bending capacity of the beam including the specified safety of the resistance side according to the EC-2. These latter values give the degree of utilizability of the specimen in a real load-bearing structure. The moment curves belonging to the different loading steps and the level of the cracking moment given in *Table 3* are shown in *Fig. 6*.

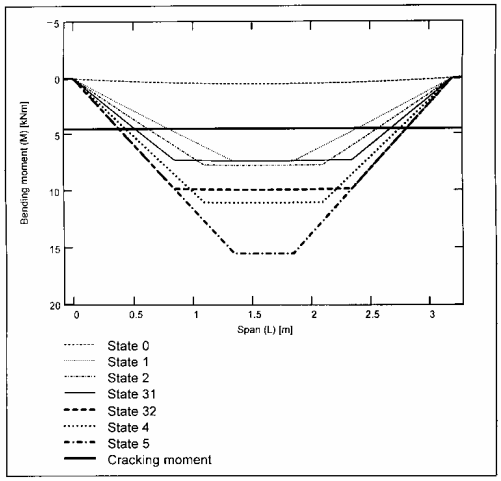

Fig. 6. Moment curves belonging to the deterioration states

Two types of excitation having different amplitude-frequency functions were applied in order to analyse their effects on the numerical values of the natural frequencies. By changing the revolution of the exciter (*Fig. 5*) during the harmonic excitation, resonance effects appeared as suddenly-increasing, relatively high peak amplitudes in the acceleration-time function. The second type of excitation was an impact effect performed by a rubber-covered hammer at approximately one-fourth of the span.

General course of the experiment was the following. First the loading step *i* had been applied to the beam producing the appropriate cracking state in it then the deflection was registered at the midspan. After the loads had been removed,

the residual deflection was also registered then the dynamic measuring phase took place determining the natural frequencies on the basis of the harmonic as well as the impulse excitation. Then the next loading step $(i + 1)$ followed with changed position and value of acting forces according to *Table 4*.

During the dynamic measuring phase, the signs of vibration got through the acceleration detector to an analyser, which recorded the acceleration-time $(A - t)$ function and immediately made a Fourier-transformation on it directly producing its amplitude spectrum. Individual parts of the recorded acceleration-time functions (containing the expected resonance effects for harmonic excitation) were saved together with their amplitude spectrums. Approximately 30 individual amplitude spectrums have been registered in each deterioration state for both types of excitation. The natural frequencies belonging to the different deterioration states have been calculated in statistical way as values equal to the average value of frequencies belonging to the maximum ordinates of the individual amplitude spectrums.

2.3. *Results*

The evaluation of the amplitude spectrums resulted in the values of the first and the second natural frequency given in *Table 5* for the different deterioration states. The last column of the table shows the difference in percentage between the first natural frequencies determined from the harmonic and the impulse excitation.

Table 5. Values of the first natural frequency

Mark of the deterioration state	*Natural frequencies* determined from				$(f_1^i - f_1^h)/f_1^h \times 100$ [%]
	harmonic excitation		impulse excitation		
	f_1^h [Hz]	f_2^h [Hz]	f_1^i [Hz]	f_2^i [Hz]	
0	36.240	134.231	36.380	136.920	0.39
1	32.300	127.952	32.329	128.799	0.09
2	31.905	127.153	31.942	128.151	0.12
31	31.779	125.126	31.928	127.051	0.47
32	30.896	123.123	31.061	123.812	0.53
4	30.636	118.425	30.692	120.924	0.18
5	30.399	117.698	30.532	120.884	0.44

As shown in *Table 5*, the decreasing tendency of the first natural frequency through the different deterioration states was similar to that of the second natural frequency for both types of excitation. The total decrease in f_1 and f_2 through the full deterioration process (between the deterioration states number 0 and 5) resulted in 16% and 12% respectively for both types of excitation. Additionally, the values got from the harmonic excitation (f_1^h, f_2^h) were always lower than the

corresponding values got from the impulse excitation (f_1^i, f_2^i) in each deterioration state. The difference between the first natural frequencies obtained from the two types of excitation was always lower than 0.6% in each deterioration state.

In the followings, the degree of deterioration will be represented by the degree of cracking and by the strain energy of internal forces, both calculated on the basis of the material and loading properties given in *Tables2*, *3* and *4* and on the equations of the EC-2. The change in the first natural frequency will be drawn as a function of the above quantities characterizing the degree of cracking. The comparison of the calculated and the corresponding measured values of the deflection at midspan will be used as a check and, as a consequence, to prove the adequacy of the above calculated quantities.

2.3.1. Analytical Investigations

As a simple, preliminary theoretical investigation, the first and the second natural frequencies of the tested specimen have been calculated by analytical expressions using the assumption that the tested specimen is uncracked along the full length of the beam as follows:

$$f^I_{1,\,\mathrm{calc}} = \frac{1}{2\pi}\pi^2\sqrt{g\frac{E_{cm}I_I}{g_0L^4}} = 33.913\ \mathrm{Hz} \tag{a1}$$

and

$$f^I_{2,\,\mathrm{calc}} = \frac{1}{2\pi}4\pi^2\sqrt{g\frac{E_{cm}I_I}{g_0L^4}} = 135.652\ \mathrm{Hz}, \tag{a2}$$

where:

$g = 9.81\ \mathrm{m/s^2}$,
$g_0 = 0.39\ \mathrm{kN/m}$ is the self-weight of the specimen,
$I_I = 5.73 \times 10^7\ \mathrm{mm^4}$ is the moment of inertia of the specimen in the plane of bending based on uncracked section,
E_{cm} is the short-term modulus of elasticity according to *Table2*.

Using the (a1) and (a2) formulae and assuming cracked sections ($I_{II} = 5.70 \times 10^6\ \mathrm{mm^4}$ instead of I_I) along the full length of the specimen, the results were $f^{II}_{1,\,\mathrm{calc}} = 10.699$ Hz and $f^{II}_{2,\,\mathrm{calc}} = 42.796$ Hz for the first and the second natural frequency, respectively.

The difference between the calculated values based on uncracked sections (*Eq.* (a1) and *Eq.* (a2)) and the measured values given in *Table 5* corresponding to the deterioration state number 0 (where no crack was observed) was not greater then 7% and 1% for the first and the second natural frequency, respectively. As shown, the calculated natural frequencies based on the fully cracked specimen ($f^{II}_{1,\,\mathrm{calc}}$, $f^{II}_{2,\,\mathrm{calc}}$)

were much lower than the measured values corresponding to the deterioration state number 5, in which the most intensive cracking state of the specimen was produced. This verifies that the use of the moment of inertia (I_{II}) based on the fully cracked specimen is not suitable for the estimation of the natural frequencies of a cracked specimen subjected to pure bending.

2.3.2. *Examination of Cracking*

The average crack width (w_{cr}) was calculated at the middle section by multiplying the average final crack spacing (s_{rm}) and the mean strain in the reinforcement (ε_{sm}) as follows. The effect of tension stiffening was taken into account and included in ε_{sm}. The numerical results based on the mean values of the material properties (*Table 2*) and the real geometric sizes of the cross section (*Table 1*) can be found in *Table 6*.

$$w_{cr} = s_{rm}\varepsilon_{sm} \tag{1}$$

with

$$s_{rm} = 50 \text{ mm } + 0.25k_1k_2\phi/\rho_r \tag{2}$$

and

$$\varepsilon_{sm} = \varepsilon_{smr} + \frac{\sigma_s}{E_p}\zeta, \tag{3}$$

where:

k_1 = 0.8 for high bond reinforcing bars,
k_2 = 0.5 for pure bending,
ϕ is the diameter of the reinforcing bar according to *Fig. 3*,
ρ_r = $A_s/(b_t h_t)$,
A_s is the total cross section of reinforcement in tension according to *Fig. 3* and *Fig. 4*,
ε_{smr} is the steel strain calculated on the basis of uncracked section subjected to the cracking moment (M_{cr}) according to *Table 3*,
σ_s is the steel stress calculated on the basis of cracked section subjected to the bending moments shown in *Fig. 6*,
E_p is the modulus of elasticity of steel,
ζ is the distribution factor taking into account the effect of tension stiffening as follows:

$$\zeta = 1.0 - \beta_1\beta_2\left(\frac{\sigma_{sr}}{\sigma_s}\right)^2 \tag{4}$$

where:

β_1 = 1.0 for high bond reinforcing bars,
β_2 = 1.0 for a single, short term loading,
σ_{sr} is the steel stress calculated on the basis of cracked section subjected to the cracking moment (M_{cr}) according to *Table 3*.

Table 6. Crack widths at the middle section and the total cross section of cracks

Mark of the deterioration state	Crack width w_{cr} [mm]	Total cross section of cracks A_{cr} [mm^2]
0	0	0
1	0.513	327
2	0.555	475
31	0.509	524
32	0.793	886
4	0.911	904
5	1.333	1176

The relationship between the crack width at the midspan and the first natural frequency is shown in *Fig. 7.a*. The greatest decrease in the first natural frequency came out between the deterioration states number 0 and number 1, simultaneously with the appearance of the first cracks. Parallel to the increase of the crack width, the first natural frequency generally decreased but in the higher domains of crack width, the intensity of this decrease became smaller.

As the crack width decreased between the deterioration states number 2 and number 31 owing to the smaller bending moment in state number 31, only the crack width at the midspan was unable to characterize the change of the natural frequency during the full deterioration process. For this reason, a new quantity, the total cross section of cracks (A_{cr}) has been defined according to *Fig. 8* as follows.

$$A_{cr} = \sum_{L_{cr}} \frac{s_{cr,i}}{s_{rm}} \frac{h_{cr,i} w_{cr,i}}{2}, \tag{5}$$

where $s_{cr,i}$ was the a distance along L_{cr} on which the averaging of h_{cr} and w_{cr} took place. It depends both on the total number of cracks in the whole beam and on their widths. The values of A_{cr} can be found in *Table 6*, the relationship between A_{cr} and the first natural frequency are shown in *Fig. 7.b*. The shape of this curve was similar to that shown in *Fig. 7.a* but this was a monotonic decreasing function. In addition, all the damages in the whole beam are included in A_{cr} while w_{cr} only belongs to a cross section.

Fig. 7.c shows the same relationship in natural logarithm scale. Because of singularity problems, the value of A_{cr} in the deterioration state number 0 was taken to a very small value (3.0 mm) instead of zero according to *Table 6*. Using the

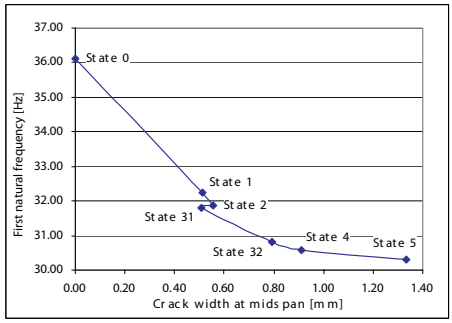

Fig. 7.a. Relationship between cracking and the first natural frequency

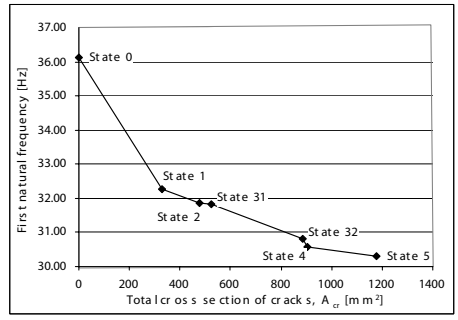

Fig. 7.b. Relationship between cracking and the first natural frequency

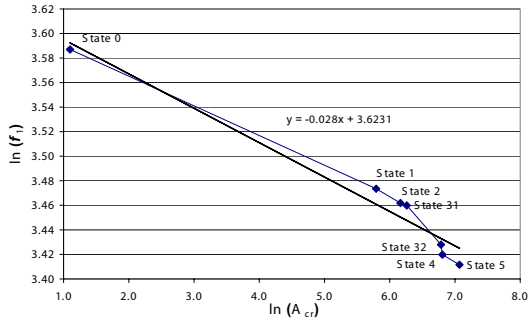

Fig. 7.c. Relationship between cracking and the first natural frequency

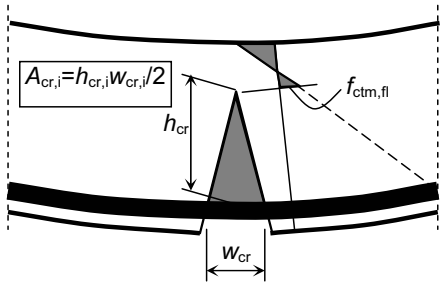

Fig. 8. Cross section of a crack

least square method, an approximating line has been fitted to the $\ln(A_{cr}) - \ln(f_1)$ function. As shown, the slope of the decreasing $\ln(A_{cr}) - \ln(f_1)$ function changed in the highest degree when the degree of utilization was increased according to *Table 4* (between deterioration states number 31 and 32).

2.3.3. *Approach Based on the Strain Energy of Internal Forces*

This approach is based on the assumption that the degree of damage in a concrete beam without prestressing and subjected to bending is proportional to the strain energy caused by internal bending moments greater than the cracking moment in non-linear elastic, cracked stage. The behaviour of a cross section subjected to bending moment less than the cracking moment is assumed to be linear elastic before the appearance of the first cracks that is no damage and no change in the bending stiffness occurs in this stage.

The mentioned strain energy was calculated along the distance of L_{cr} in each deterioration state as follows:

$$W = \int_{L_{cr}} M(x)\rho(x)\,\mathrm{d}x, \tag{6}$$

where $M(x)$ was the bending moment function according to *Fig. 6* and $\rho(x)$ was the curvature function taking into account the effect of tension stiffening by $\zeta(x)$ according to *Eq.* (4) as follows:

$$\rho(x) = \zeta(x)\frac{M(x)}{E_{cm}I_{II}} + [1-\zeta(x)]\frac{M(x)}{E_{cm}I_{I}}, \tag{7}$$

where I_I and I_{II} were the moments of inertia of the cross section in uncracked and cracked stage, respectively and x was the length measured along the tested specimen. The $\rho(x)$ curvature function and the $M(\mathrm{x})\rho(x)$ function-product can be seen in *Fig. 9.a* and *9.b* for the different deterioration states based on the mean values of the material properties and the real geometric sizes of the cross section.

The strain energy according to *Eq.* (6) was represented by the area under the functions shown in *Fig. 9.b* along the length of L_{cr}. The numerical values can be found in *Table 7*.

Table 7. Strain energy along the cracked sections

Mark of the deterioration state	Strain energy W [kNmm]
0	0
1	198.9
2	317.9
31	339.5
32	793.9
4	855.8
5	1504.7

The relationship between the strain energy and the first natural frequency is shown in *Fig. 10*. As shown, the shape of this curve was similar to that shown in

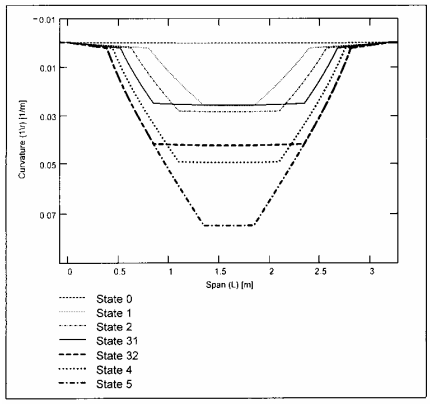

Fig. 9. a

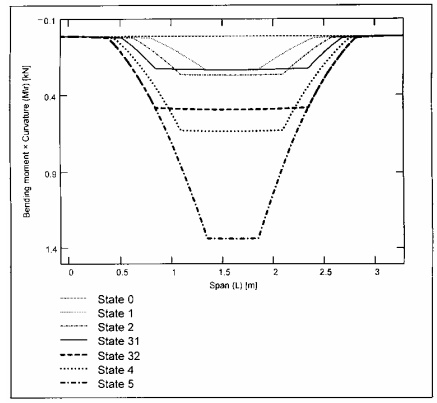

Fig. 9.b

Relationship between the strain energy and the first natural frequency

Fig. 7.b since it was derived from the same input parameters (bending moments and cross sectional properties).

Fig. 10.b shows the same relationship in natural logarithm scale. Because of singularity problems, the value of W in the deterioration state number 0 was taken to a very small value (3.0 kNmm) instead of zero according to *Table 7*. Using the least square method, an approximating line with its function has been fitted to the $\ln(W) - \ln(f_1)$ function. As shown, both the slope and the whole function of the approximating line was almost the same as in *Fig. 7.c*. In this case, a more perfect fitting could be observed compared to that in *Fig. 7.c*.

2.3.4. Deflections

Table 8 contains the deflection values measured at the middle section of the beam under loading and after load relief in each deterioration state (*Fig.5*). *Table 8* also contains the calculated deflections (e_{calc}) based on the mean values of the material properties (*Table 2*) and the real geometric sizes of the cross section (*Table 1*). These values have been calculated by *Eq.* (1) where $\rho(x)$ is according to *Eq.* (7) and *Fig. 9.a*. Furthermore φ is the rotation of the section above one of the supports and x is the distance along the beam measured from the same support. The e_{measured} values are always referred to the beam axis subjected to the residual deformations caused by the previous loading steps. Therefore *Table 8* also contains the total deflections (e_{tot}) including the current measured as well as the previous residual deformations.

$$e_{\text{calc}} = \varphi \frac{L}{2} - \int_0^{L/2} \rho(x) \left(\frac{L}{2} - x \right) \mathrm{d}x \tag{8}$$

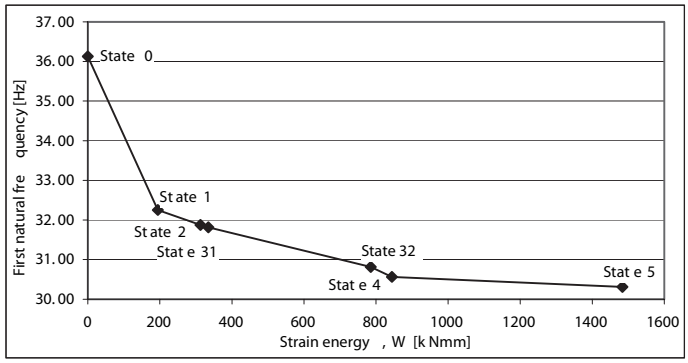

Fig. 10.a Relationship between the strain energy and the first natural frequency

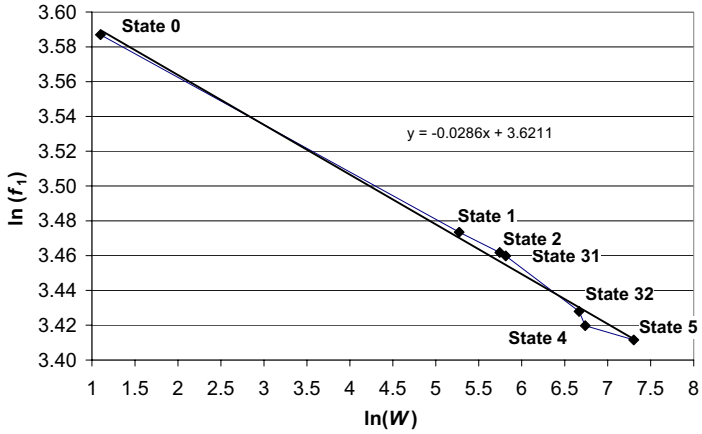

Fig. 10. b Relationship between the strain energy and the first natural frequency

The more important deflection values given in *Table 8* are also presented in *Fig. 11*. As shown, the calculated and the measured deflections under loading were very close to each other in the lower domains of utilization for bending (*Table4*). However in the higher domains, the calculated values were significantly greater than the measured deflections. This fact can be explained mainly by the calculation model of $\zeta(x)$ and by the residual deformations and internal stresses in the beam caused by previous loadings. The ζ factor surely underrates the effect of tension stiffening of concrete in the higher domains of utilization because of the quadratic relation in *Eq.* (4), which generally results in higher deformation values, while in the lower domains, it probably provides a closer approximation of the real behaviour.

Considering the curves in *Fig. 11* corresponding to the measured and the calculated deflections between the deterioration states number 0 and 32 a very close coincidence can be observed, which proves the adequacy of the previous calculated data in connection with the cracking states of the beam.

Table 8. Measured and calculated deflections

Mark of the deterioration state	$e_{measured}$ [mm]		e_{tot} [mm]		e_{calc} [mm] under loading
	under loading	after load removal	under loading	after load removal	
0	0	0	0	0	0.275 (self-weight)
1	21.12	7.72	21.12	7.72	19.07
2	19.61	0.83	27.33	8.55	26.04
31	19.80	1.14	28.35	9.69	26.74
32	32.27	3.11	41.96	12.80	45.74
4	28.75	0.91	41.55	13.71	48.46
5	22.73	0.77	36.44	14.48	67.44

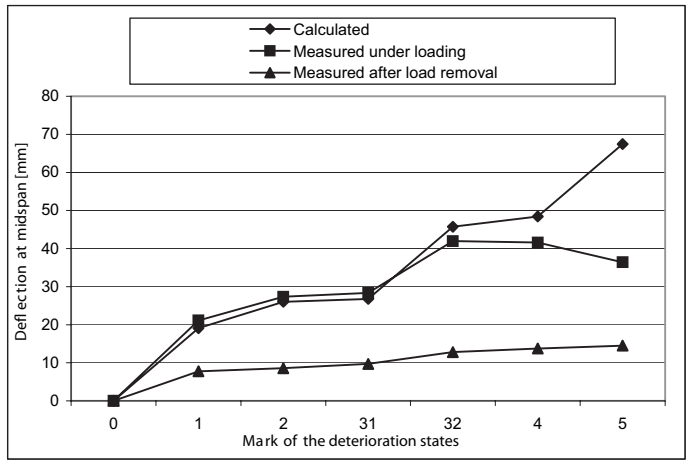

Fig. 11. Measured and calculated deflections at the middle section

2.4. Summary of the Laboratory Test

In the framework of the targeted research programme, which aims to develop conditions for the continuous monitoring of concrete bridges during their design lifes, laboratory test of a lightly reinforced concrete beam has been carried out. The tested specimen has been investigated under artificially produced cracking states made by a four-point bending test. The artificially produced cracking states modelled a gradually developing deterioration process in the structure from the uncracked state up to the bending failure. The goal was to point out a numerical relationship between the first natural frequency and the quantities characterizing the degree of damage accumulated in the specimen.

In this case, the damage was measured by the degree of cracking. The quantities characterizing the cracking states were calculated by the expressions of the EC-2 and were checked by the comparison of the calculated and the measured values of the deflection.

For the dynamic measurements, harmonic and impulse excitations were used. The numerical values were derived from statistical analysis. The results of the test can be summarized as follows:

- It was pointed out that for reinforced concrete specimens subjected to pure bending neither the moment of inertia nor the crack width at a particular point of the specimen can be used as damage identification parameter because they belong to a cross section, i.e. they are unable to measure the damage accumulated in the whole beam. For this reason, two possible damage identification factors – the total cross section of cracks and the strain energy – have been calculated by a detailed analysis of the cracked length of the tested specimen.
- The measured changes in the first natural frequency during the deterioration process were demonstrated as the functions of the above damage identification factors. The first natural frequency simultaneously decreased with the increase of the damage identification factors. Tendency of decreasing was monotonic during the full damage accumulating process. Highest intensity of decreasing could be observed when the first cracks appeared then this intensity became smaller in states close to failure. Applying a log-log scale description for these relationships and a linear curve (line) fitting to the resulting function, approximately the same linear function could be obtained for both damage identification factors, what was able to characterize the degree of damage numerically.
- As a quantitative characterization of the investigated, full deterioration process, the maximum changes in the first and the second natural frequency were 16% and 12%, respectively between the extreme states of deterioration.
- It has to be taken into account that the cracking behaviour of the reinforced concrete elements can be significantly influenced by the applied amount of reinforcement as well as by application of prestressing. The next steps of the intended research programme should focus on these parameters.

References

[1] ILLÉSY, J., On the Investigation for Condition by Easily Reproducible Dynamic 'In-situ' Short-Time Measurements, *Report on The 9th International Congress of the FIP*, Stockholm, Sweden, June 6–10, 1982.

[2] ILLÉSY, J., Continuous Testing of R.C. Structures' Overall Behaviour by Means of Their Natural Frequencies, *Testing in situ II*, RILEM, 1977. pp. 90–100.

[3] CASAS, J. R., An Experimental Study on the Use of Dynamic Tests for Surveillance of Concrete Structures, *Materials and Structures*, **27** (174) (1994), pp. 588–595.

[4] CASAS, J. R. – AAPARICIO, A. C., Structural Damage Identification from Dynamic Test Data, *Structural Engineering*, **120** (8) (1994), pp. 2437–2450.

[5] SALAWU, O. S. – WILLIAMS, C., Bridge Assessment Using Forced-Vibration Testing, *Structural Engineering*, **121** (2) (1995), pp. 161–172.
[6] GUDMUNSUN, P., The Dynamic Behaviour of Slender Structures with Cross-Sectional Cracks, *Mechanics and Physics of Solids*, **31** pp. 329–345.
[7] KÁLLÓ, M., A Simple Measuring Method for the Determination of Natural Frequencies and Eigenfunctions of Bridges – Dynamic Investigations on Bridges, *Publication of the Széchenyi István College*, Scientific Workshop, Győr, May 1996, pp. 1–6.
[8] KOVÁCS, T. – FARKAS, GY. – KÁLLÓ, M., Examination of Dynamic Characteristics of Reinforced Concrete Bridges, *Scientific Publications of the Department of Reinforced Concrete Structures, Technical University of Budapest*, Műegyetemi Kiadó, Budapest, 1998, pp. 111–124.
[9] KOVÁCS, T., Measurement of Structural Damping on Existing Concrete Bridges, *Scientific Publications of the Department of Reinforced Concrete Structures, Technical University of Budapest*, Műegyetemi Kiadó, Budapest, 1999, pp. 175–186.
[10] FARKAS, GY. – KOVÁCS, T., The Assessment of Damage by Dynamic Characteristics, *Proceedings of the 4th Int. Conference on Bridges Across the Danube*, Bratislava, Slovakia, 13–15 September, 2001, pp. 217–222.
[11] KOVÁCS, T. – FARKAS, GY., The Assessment of Damage by Dynamic Characteristics on Model Beams, *Proceedings of the 3rd International PhD Symposium in Civil Engineering*, Vienna, 5–7 October 2000, Vol. 1, pp. 297–306.